Available online at www.sciencedirect.com
ScienceDirect
Journal of the European Ceramic Society 28 (2008) 455–463
www.elsevier.com/locate/jeurceramsoc

Growth of textured mullite fibers using a quadrupole lamp furnace

W. Yoon, P. Sarin, W.M. Kriven *

Department of Materials Science and Engineering, University of Illinois at Urbana-Champaign, 1304 W. Green Street, Urbana, IL 61801, United States

Available online 4 June 2007

Abstract

Fine ceramic oxide fibers are widely used as reinforcements in composites for high temperature applications. The primary goal of this research was to investigate the growth of single crystal or textured oxide fibers by heat treatment of polycrystalline or amorphous, extruded precursor fibers. Mullite was selected for this study due to its excellent chemical stability, creep resistance and strength at high temperatures. A quadrupole lamp furnace (QLF), with a small, disc-shaped, hot zone was used for the heat treatment.

Micrographic analysis and *in situ* synchrotron X-ray diffraction analysis have been performed on the mullite system for anisotropic grain growth of mullite. The estimated activation energies from the SEM micrographic analysis were 644.3 and 773.7 kJ/mol for the length and thickness, respectively. An *in situ* synchrotron X-ray diffraction microstructure analysis was done with a curved image plate (CIP) detector and the fiber was heat treated with a QLF. A Williamson–Hall analysis was carried out for the calculation of the apparent crystallite sizes. The apparent crystallite size showed anisotropy in crystallite growth. Furthermore, the growth rates in the [0 0 1] and [1 1 0] directions demonstrated elongated crystallite growth.

Mullite whiskers were prepared by HF leaching out and templated into polycrystalline mullite fiber by extrusion. Textured growth of mullite fiber with elongated grains, ~400 μm in length and aligned along the long-axis of the fibers, was achieved by heat treatment. Repeated heat treatment cycles of a whisker-templated fiber showed a bamboo-like microstructure. It was confirmed by TEM that the growth direction along the fiber length was the [0 0 1] direction of orthorhombic mullite.

Keywords: Grain growth; Fibers; Mullite; Synchrotron XRD

1. Introduction

Small diameter oxide fibers are excellent reinforcements for composites for use in high temperature applications.[1] Mullite is a strong candidate material for advanced structural applications at high temperature, because of its low thermal expansion, low thermal conductivity, good chemical and thermal stability, high temperature strength, and creep resistance.[2–4] Several techniques have been reported to synthesize mullite fibers and whiskers for ceramic composite reinforcements. As the ceramic shows reduced mechanical properties with grain growth, the anisotropic grain growth of a mullite system has been explored to develop a three-dimensionally interpenetrating, acicular, grain microstructure.[5]

Single crystal or textured, oxide fibers exhibit better properties than do amorphous or polycrystalline oxide fibers. Crystallization and synthesis of mullite fibers have been studied by different methods.[6–10] Polycrystalline ceramic fibers have less creep resistance in comparison to single crystal or textured fibers, due to the presence of flaws and the tendency to creep along grain boundaries at high temperatures.

Densification and grain growth kinetics of mullite ceramics were first investigated by Ghate et al.[11] They assumed that diffusion of Si^{4+} ions controlled densification and grain growth. Huang et al.[12] reported that the grain size evolution of mullite is slow below 1590 °C and that equiaxial grains remain. Above 1590 °C, the equiaxed mullite grains became acicular. They explained this elongated anisotropic grain growth as being due to enhanced diffusion in the presence of a liquid silicate phase that forms above 1590 °C, in the case of silica-rich mullite. Anisotropic grain growth of mullite has been reported in

* Corresponding author. Tel.: +1 217 333 5258; fax: +1 217 333 2736.
E-mail address: kriven@uiuc.edu (W.M. Kriven).

0955-2219/$ – see front matter © 2007 Published by Elsevier Ltd.
doi:10.1016/j.jeurceramsoc.2007.03.019

directional solidification[13] and during vapor–solid synthesis of whiskers.[14]

Incorporation of transition metal cations into the mullite crystal structure has been studied by many researchers. Hong and Messing[15] reported the effect of titania addition on the mullite microstructure. They reported that the onset temperature for anisotropic grain growth decreased with increasing titania concentration and was very close to the point of maximum densification. Therefore, the addition of the titania enhanced the densification of a mullite sintered body.

For years many X-ray powder diffraction methods have been used in materials characterization.[16] With the development of synchrotron sources, there has been an explosive growth in X-ray diffraction methods of materials. Amongst the many advantages that synchrotron X-ray sources offer over conventional laboratory X-ray equipment, are higher photon flux, tunability of X-radiation wavelengths, and a non-divergent or parallel X-ray beam. Most commonly, X-ray diffraction data is collected using point detectors, which, together with crystal analyzers, provide the highest spatial resolution. However, measurements on samples that change in time are difficult and sometimes impossible for kinetic studies at high temperature.

A new, one-dimensional, curved image plate (CIP) detector has been developed in our laboratory and has been used for *in situ* experiments.[17] The CIP detector has a capability of detecting X-ray diffraction, particularly in terms of very high resolution to at least 0.001° in peak position, and has been designed for operation together with a quadrupole lamp furnace. This set-up has enabled *in situ* high temperature X-ray diffraction studies on polycrystalline specimens, in real time, up to 2000 °C in air. The details of the experimental apparatus and detector information have been reported in other papers.[18–22]

The primary objective of this research was to investigate the possibility of producing single crystal or textured fibers of mullite by controlled texturing or crystallization of polycrystalline or amorphous fibers as precursors. In order to produce textured fibers by extrusion, the use of mullite whiskers as templates was investigated. Precursor fibers were subjected to heat treatments in the quadrupole furnace. The effect of furnace temperature, traverse rate of the fiber through the furnace hot zone, and the number of heating cycles on microstructural modification of the fiber were studied. The nature of *in situ* crystallite size growth of the mullite system was examined on a representative statistical level by synchrotron XRD and the CIP detector.

2. Experimental procedures

2.1. Synthesis of mullite template needles

The precursor mullite fibers were prepared by an extrusion method. To obtain an aligned or bamboo structured fiber, the templated grain growth (TGG) method[23] was employed, for which mullite whiskers were prepared as templates. TGG is one of the techniques for developing textured microstructures as well as developing single crystals without melting. In TGG a small number of large, usually anisotropic, templates are aligned in a fine powder matrix during a shear forming process as shown in Fig. 1. These larger anisotropic particles grow by the consumption of the surrounding fine-grained matrix, yielding highly oriented, textured or single crystalline grains, upon heat treatment.

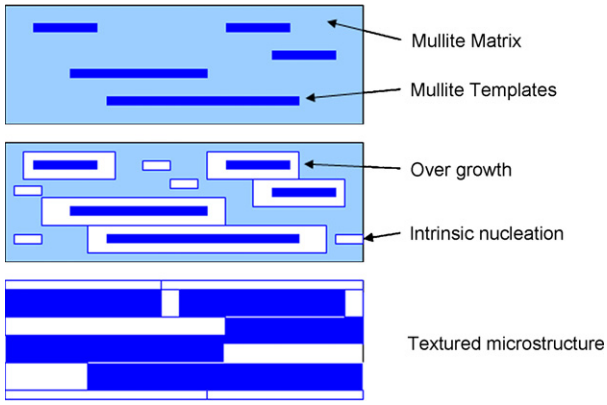

Fig. 1. Schematic of templated grain growth (TGG).

Titinia was added to the mullite system in order to enhance anisotropic grain growth. Titania-doped mullite powders were synthesized by the sol–gel method. Aluminum nitrate nonahydrate ($Al(NO_3)_3{\cdot}9H_2O$) and tetraethyl orthosilicate ($Si[OC_2H_5]_4$) were prepared as starting chemicals and dissolved in ethanol. Titanium ethoxide ($Ti[OC_2H_5]_4$) was added to the mullite sol as a source for the titanium ions. After gelation with ammonium hydroxide, the dried gel was calcined at 1000 °C for 2 h and later crystallized at 1300 °C for 2 h in a $MoSi_2$ furnace. The synthesis of mullite phase was confirmed by X-ray diffractometry.

The synthesized titania-doped mullite powder was pressed as a pellet, and sintered at 1600 °C for 15 h. Mullite whiskers were collected from a sintered mullite sample by a hydrofluoric acid leaching off reaction. The grain boundaries were removed and the elongated mullite grains were collected. Sintered pellets were crushed and soaked in 49 vol% hydrofluoric acid solution, and the resulting cloudy dispersion was repeatedly rinsed with deionized water to collect the mullite whiskers. Their shape and size were examined by SEM (Hitachi S-4700, Hitachi High Technologies America, Inc., Schaumburg, IL).

2.2. Synthesis of fibers

Mullite fibers were prepared by an extrusion method. Pure and 5 wt% whisker-templated fibers were synthesized. Commercial mullite powder (KM Mullite 101, Kyoritsu Ceramic Materials Co. Ltd., Nagoya, Japan) and the whiskers collected were used as starting precursor powders. Three weight percent aqueous hydroxypropyl methyl cellulose solution was prepared and mixed with the prepared starting precursor powder to make a viscous paste. For the templated fiber, about 5 wt% whiskers were added to the KM mullite powder. The green fibers were extruded in a fiber extruder (Marksman Fiber Drawing Machine, Chemat Technology Inc., Northridge, CA) through a 200 μm orifice. The orientation of the whiskers in an extruded fiber was

aligned along the fiber length direction, due to the high aspect ratio of the whiskers. The mullite whisker-templated green fibers were sintered at 1300 °C for 2 h and the resulting diameter was about 150 μm after sintering.

2.3. In situ crystallite size determination by synchrotron radiation

The *in situ* synchrotron experiments were carried out at Sector 33-BM, UNICAT of the Advanced Photon Source (APS), Argonne National Laboratory (ANL, Argonne, IL). A quadrupole lamp furnace (QLF) was used for heat treatment of the polycrystalline mullite fibers. Four halogen lamps (OSRAM 15 V, 10 A, Osram, Germany) with ellipsoidal reflectors were mounted in the brass furnace housing which served as a heat source. The QLF was mounted onto a Huber four-circle goniometer and the temperature was controlled with an R-type thermocouple. The furnace housing had two extra slits for the incoming synchrotron beam and for the diffracted beam. The curved image plate (CIP) detector was used for data acquisition.

The sintered, pure, polycrystalline fiber was coated with platinum paste which functioned as an internal thermometer when the fiber was heated by the image furnace. The coated fiber was attached to the alumina tube which was mounted horizontally to the goniometer stage. The fiber was rotated at 60 rpm for random diffraction and better counting statistics. The X-ray diffraction patterns were collected by the CIP detector isothermally for more than 1 h.

The XRD pattern collected with the CIP detector was compared with that collected using an analyzer with LaB_6 powder, (SRM660a, National Institute of Standards and Technology, Gaithersburg, MD) in order to assign of 2θ values to each pixel on the image plate (IP). A polynomial of second order was derived to transform the pixel values on the IP into 2θ values. The residuals of the fitting were less than 0.0002° and also showed randomness in 2θ ranges. The incident X-radiation of $\lambda = 0.700642795$ Å (approximately 17.7 keV) was used for the pattern acquisition.

The peak position and Full Width at Half Maximum (FWHM) were analyzed with the CMPR[24] program. The actual temperature of the heat treatment was calculated based on the lattice expansion of the Pt by the Rietveld whole pattern fitting method.[25] In order to correct for instrumental broadening, a standard sample diffraction pattern from LaB_6 (SRM660a) was collected and analyzed. The crystallite size, growth rate and crystallite shape were examined by applying the Williamson–Hall method.

2.4. Heat treatment of fibers

The mullite whisker templated fiber was mounted inside of the crystallizer vertically. A quadrupole lamp furnace (QLF) was employed for heat treatment of the mullite fiber. The shape and size of the furnace hot zone were determined by measurement of both the axial and radial distribution of temperature using an R-type thermocouple (Pt/Pt13%Rh). The fiber was heat treated at up to 92% of furnace power, and for several heating cycles for the microstructural evolution.

The surface morphologies of the heat treated fibers were examined by SEM (Hitachi S-4700). TEM observations were performed with 200 kV Jeol electron microscopes (JEM 2010F, JEM 2010 LaB_6, JEOL USA, Inc., Peabody, MA). A piece of fiber was mounted on a copper grid and iron milled in a Fischione Ion mill (Fischione Instruments, Inc., Export, PA). The as-heat treated fiber and ion-milled fibers were examined by optical microscopy (Zeiss Axio Imager, Carl Zeiss MicroImaging GmbH, Göttingen, Germany) in reflected and transmitted modes, using normal and plane polarized light.

3. Results and discussion

The elongated anisotropic grain growth occurring in mullite is widely known. The heat treatment of the polycrystalline mullite system showed random grain growth. In order to make an oriented mullite microstructure, the templated grain growth (TGG) method was employed. In the case of TGG, the one dimensional crystal orientation can be controlled by the alignment of the template.[26] As the heating temperature increased, equiaxed mullite grains became elongated grains as expected. The microstructure of the sintered pellet showed the elongated mullite grains in random orientation as seen in Fig. 2(a). A SEM micrograph of the mullite whiskers used as templates in this study is shown in Fig. 2(b).

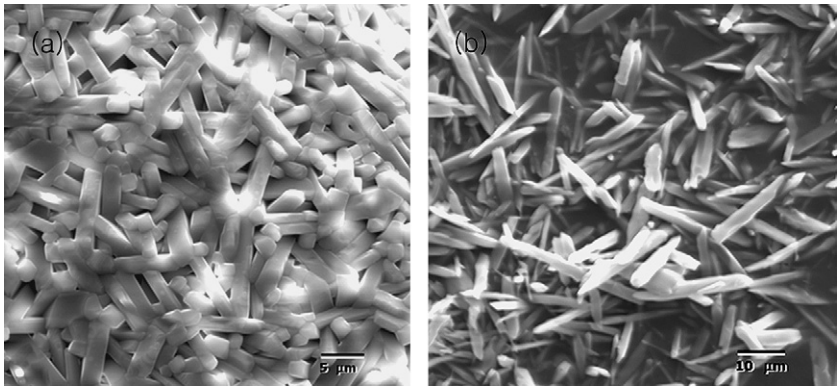

Fig. 2. (a) Mullite sintered pellet, (b) mullite whiskers collected after heat treatment at 1600 °C for 15 h.

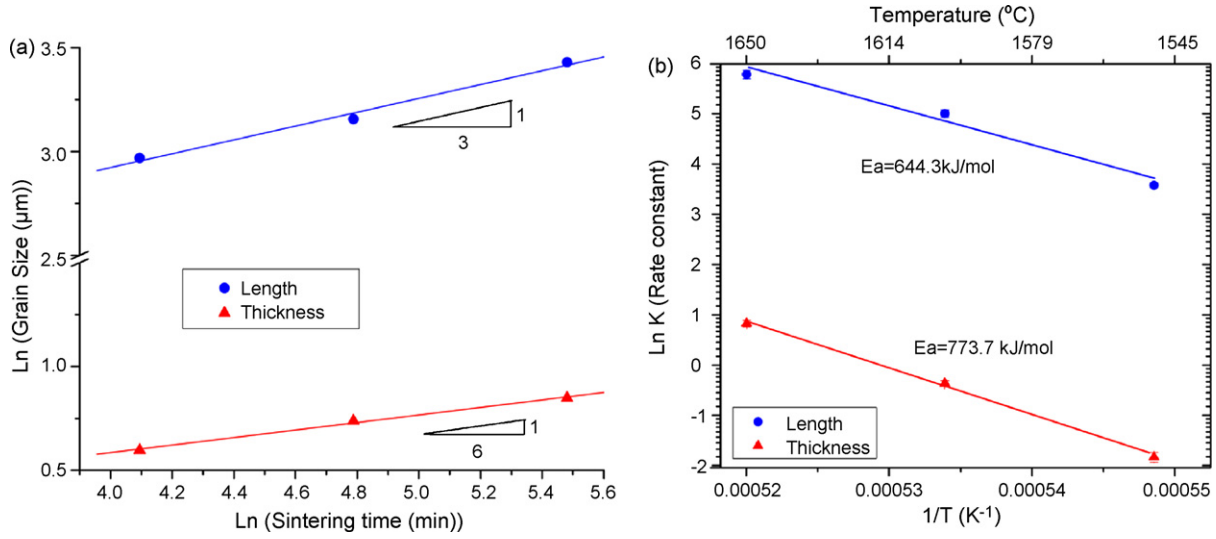

Fig. 3. (a) Anisotropic grain growth kinetics at 1600 °C, (b) Activation energies of 3 wt% titania-doped in length and thickness directions.

The mullite whiskers collected were needle-shaped and had sharp ends. The tendency for mullite grains to grow as needle shapes has been widely known, for if the grains grow without constraint they form whiskers.[14,27] When the elongated mullite grains were made, the whiskers grew in the *c*-axis and were bounded by {1 1 0} surfaces. From these results, it is believed that the prismatic planes {1 1 0} have a lower surface energy than do the other planes, and thus, grains grow in the [0 0 1] direction for thermodynamic reasons.[13–15]

The sintered body and the collected whiskers were examined by EDS and SEM. Glass pockets were commonly observed in the grain boundaries around the anisotropic grains in the sintered pellet, and EDS analysis indicated that the glassy phase consisted of Si with a small amount of Al and Ti. It was expected that there was a trace amount of titania inside of the mullite whisker as the solubility limit of titania in a mullite matrix is reported to be 2.9 wt%, and it substitutes for octahedrally coordinated Al^{3+} in mullite.[28] EDS spectra from the mullite whiskers reveals

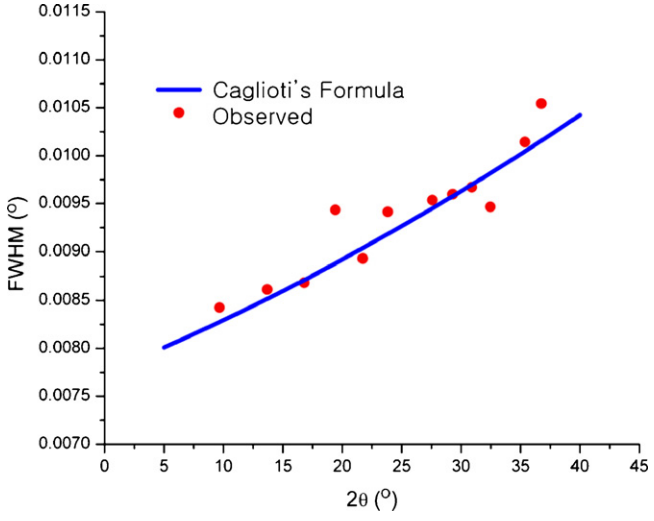

Fig. 4. Instrumental broadening with LaB_6 and Caglioti's function.

that they consisted of Al and Si. The aspect ratio, a measure of the degree of anisotropy, is an important characteristic in microstructures consisting of platelet or needle-like grains. The thickness of the mullite whiskers was about 3 μm. This aspect ratio increased with increasing titania doping and heat treatment temperature. The aspect ratio between thickness and length was about 12 for 3 wt% titania addition and heat treatment at 1600 °C for 15 h.

To determine the anisotropic grain growth kinetics, the grain length, grain thickness, and aspect ratio were measured for the 3 wt% titania-doped mullite. The grain growth kinetics of equiaxed grains can be expressed by the following empirical equation:[29]

$$G^n - G_o^n = Kt \quad (1)$$

where G is the grain size, G_o the initial grain size, K the rate constant, and t is the time. This model assumes that the mobility of the grain interface was constant during growth in all crystallographic planes of the interface. The value of the exponent n depends on the grain growth mechanism; $n = 2$ for reaction-controlled and $n = 3$ for diffusion-controlled grain growth.[29] The exponent n for grain growth could be determined from the slope of the log–log plots of grain size *versus* time as seen in Fig. 3(a). The exponent for the length direction was 3 and for the thickness it was 6. The cubic growth kinetics in the length direction can be interpreted as being due to diffusion-controlled growth in the liquid. The growth kinetics in the thickness direction was much slower than in the length direction.

As the grain growth is a thermally activated process, the rate constant can be expressed in the Arrhenius form. The activation energy for the gain growth can be calculated from the slope of the plot of $\ln K$ *versus* $1/T$ as seen in Fig. 3(b). The estimated activation energies were 644.3 ± 40.2 and 773.7 ± 29.8 kJ/mol for the length and thickness, respectively. These results indicate that the growth rate in the length direction is much faster than in the thickness direction. The large differences of roughness in the solid/liquid interface and different growth mechanisms

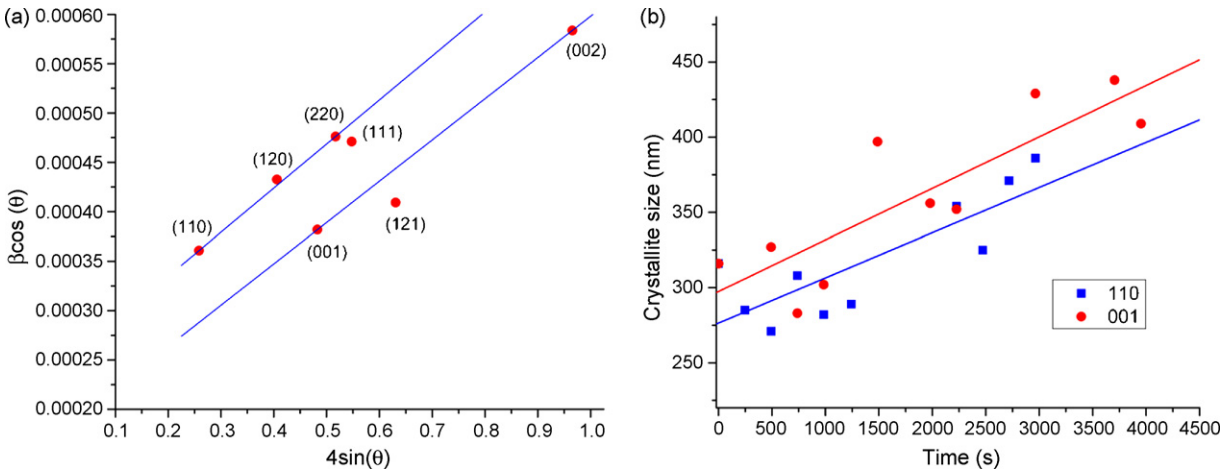

Fig. 5. (a) Williamson–Hall plot of mullite for crystallite size, (b) crystallite growth rate in different crystallographic directions at 1589 °C.

in each direction for Si_3N_4 system were explained by Hwang et al.[30] and Lai et al.[31] The relative roughness of interfaces in each direction is closely related to the anisotropic grain boundary energy, which is related to the mullite crystal structure.[32] Thus, anisotropic grain growth behavior in titania-doped mullite is due to the intrinsic, anisotropic crystal structure in which strongly bonded chains lie along the *c*-axis. In addition, titania doping provides an extrinsic environment of low-viscosity for constraint-free growth. The local titania distribution strongly affects the initiation of anisotropic grain growth due to the formation of local regions of lower viscosity near each particle. This local chemical heterogeneity leads to the initiation of anisotropic grain growth of mullite grains.[15]

The anisotropic crystallite growth was also studied by *in situ* synchrotron X-ray diffraction (XRD) experiments. The microstructure examined by XRD came from crystallites having coherent diffraction domains. These domains can be understood as the submicrostructure which forms grains by a mosaic of crystallites.[33]

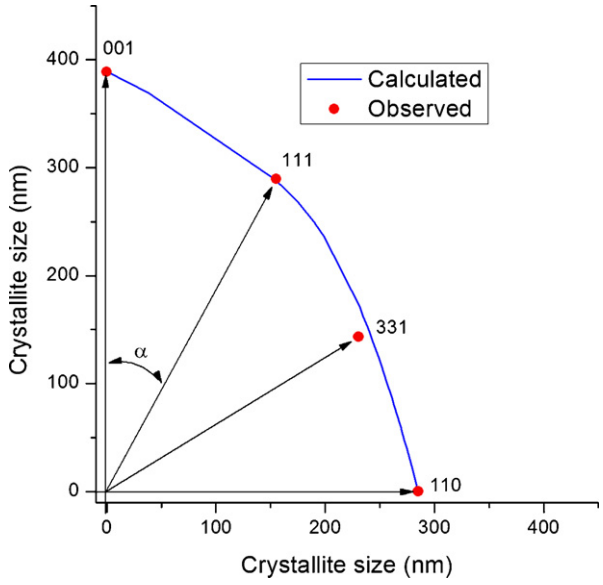

Fig. 6. Polar plots of crystallite size as a function of crystallographic direction.

In order to determine the structural imperfections and the morphology of the mullite crystallites, the breadths of all accessible Bragg reflection lines were required. Pattern decompositions of the acquired XRD patterns were carried out by means of the profile-fitting program CMPR[24] for the individual peaks. Line profiles were assumed to be pseudo-Voigtian and thus described by their position, integrated intensity and full width at half maximum (FWHM), in addition to the mixing parameter ε, which related the Lorentzian and Gaussian contributions to the pseudo-Voigt function. Also, the integral breadths β of the each peak were calculated from the peak intensity and peak height.

The FWHM of the standard sample peak is shown in Fig. 4. It is evident that peak broadening depends on $(h\,k\,l)$ indices, since the apparent scatter is much greater than that due to random errors. The instrumental broadening was corrected with the Caglioti's formula:

$$\mathrm{FWHM}^2 = U\tan^2(\theta) + V\tan(\theta) + W \quad (2)$$

From Fig. 4, the U, V, and W values were calculated by least squares fitting. The instrumental broadening was corrected

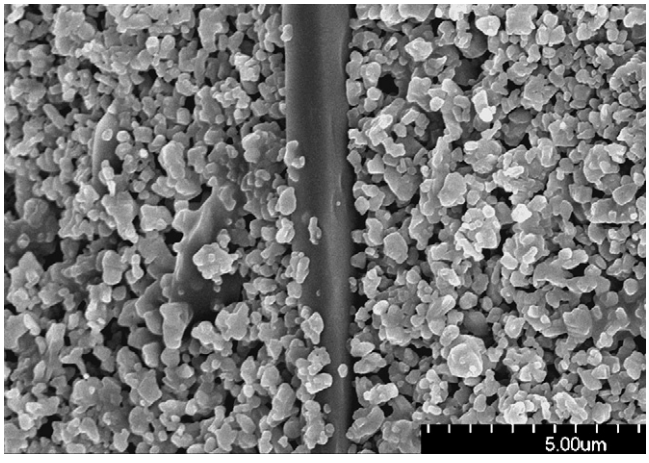

Fig. 7. Mullite whisker embedded along the fiber length in precursor fiber after extrusion.

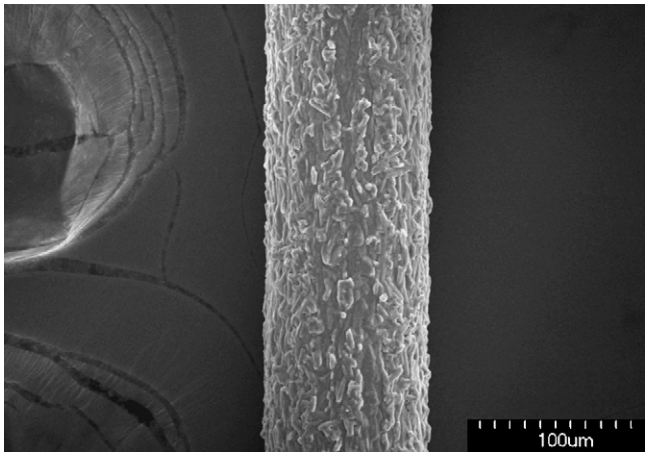

Fig. 8. SEM micrograph of extruded 5 wt% whisker added mullite fiber at 89% of power (approximately 1810 °C), at a transverse rate of 1 μm/s.

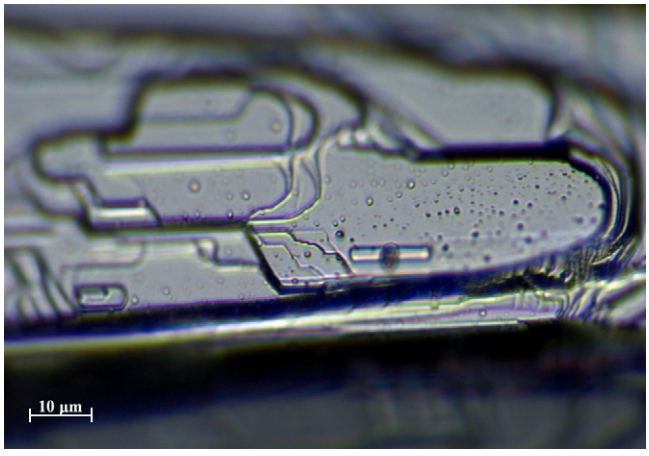

Fig. 10. Optical micrograph of whisker-templated mullite fiber heat-treated 10 times at 85% of power (approximately 1780 °C), at a transverse rate of 1 μm/s in reflection mode.

using Caglioti's formula, where the constants for the Caglioti's formula were 0.00012, 0.00009, and 0.00006, respectively.

In this study the Williamson–Hall method which is one of the integral breadth methods, was used for the crystallite size analysis.[34] The Williamson–Hall plot ($\beta\cos(\theta)$ *versus* $4\sin(\theta)$) is useful for a first-look estimation of the nature of structural imperfections present in a sample. If all values of $\beta\cos(\theta)$ lie on a horizontal line, then the strain broadening is negligible and the crystallites are equiaxed on average. When the values of $\beta\cos(\theta)$, corresponding to different reflection groups, lie on several horizontal lines, the strain broadening is again negligible but the crystallite shape is not equiaxed. The size and strain parameters can be estimated by means of the Williamson–Hall plot, by applying the following approximate formula:

$$\beta\cos(\theta) = \frac{\lambda}{D} + 4\varepsilon\sin(\theta) \quad (3)$$

where D is the apparent crystallite size and ε is the strain parameter.

A set of the Williamson–Hall plots was produced for analyzing the corrected line profiles corresponding to the mullite reflections from all samples as in Fig. 5(a). Two parallel straight lines, corresponding to two pairs of reflections of different orders (each of them corresponding to the same direction, 1 1 0–2 2 0 and 0 0 1–0 0 2), were constructed for each plot by taking the same slope of both the lines and using least-squares fitting. In all samples the anisotropies of the crystallite sizes (in different directions) were observed. These results agreed with the known fact that the growth of mullite crystallites is frequently anisotropic. The calculated crystallite sizes were 285 and 389 nm in [1 1 0] and [0 0 1] crystallographic directions, respectively.

The actual temperature of the experiment can be acquired from the Rietveld whole pattern fitting of the platinum internal thermometer. As the platinum is stable at high temperatures and has cubic symmetry, the actual temperature can be calculated from the lattice expansion of the platinum. The actual calculated temperature was 1588.7 ± 8.6 °C for the set temperature of 1300 °C and the Pt lattice constant was 3.99292 ± 0.00051 Å. The calculated crystallite sizes were much smaller than the mullite grains in SEM micrographs in Fig. 2. It was because the heat treatment time was different. In the case of Fig. 2, the mullite sample was heat treated for 15 h. Also it is thought that the calculated crystallite size was the size of submicrostructure of a mosaic of crystallites.

The series of X-ray diffraction patterns was collected isothermally at set temperature of 1300 °C for 4000 s. The crystallite sizes in [1 1 0] and [0 0 1] directions were calculated from Williamson–Hall plots. The growth rate along [1 1 0] and [0 0 1] directions were 0.030 and 0.034 nm/s, respectively as seen in Fig. 5(b). As expected the growth rate along the [0 0 1] direction was higher than along the [1 1 0] direction.

The apparent crystallite sizes as a function of the angle α between the diffraction vector and the c-axis of the mullite unit

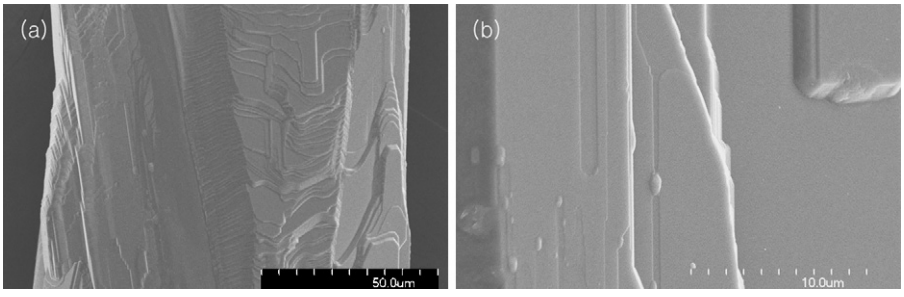

Fig. 9. (a) SEM micrographs of extruded 5 wt% whisker added mullite fiber heat treated 10 times at 85% of power (approximately 1780 °C), at a transverse rate of 1 μm/s, (b) high resolution of (a).

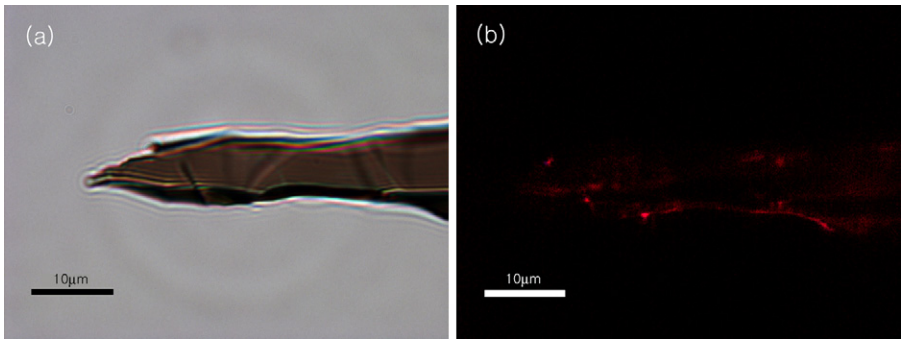

Fig. 11. Optical micrograph of heat treated fiber (a) in transmission mode, (b) total extinction in transmitted polarized light.

cell were plotted. The Fig. 6 shows the elongated shape of the crystallites. The curve in the diagram was calculated from the cylindrical parameters and shows the dependence of apparent crystallite size on lattice direction. The lengths of the line segments indicated the experimental values of apparent crystallite size as obtained from the analysis.

It is thought that textured microstructure development during templated grain growth is controlled by the growth of the template particles, rather than by template rearrangement or preferential development of texture in the matrix.[35,36] Alignment of whiskers in the precursor fiber was along the fiber length direction as in Fig. 7. As the elongated whiskers passed through the small orifice in the fiber extruder, the whiskers were aligned along the fiber length direction due to the shear. With heat treatment there was over-growth around the templates with the absorption of small mullite grains into the large elongated grains, as expected.

The SEM micrograph in Fig. 8 shows the microstructure of heat-treated 5 wt% whisker-templated fiber. The heat treatment was carried out at 89% of power (approximately 1810 °C) at 1 μm/s of transverse rate. The large elongated mullite grains along the fiber length direction grew with each heat treatment. Elongated grains over 400 μm in length were also observed. In this case the aspect ratio was over 40. During the heat treatment cycle, a considerably textured microstructure was achieved, although some randomly oriented grains were still present. Raj et al.[37] predicted that oriented grains with aspect ratios of 50 increased the creep resistance by a factor of 10^5 relative to randomly oriented equiaxed grains.

Therefore, the fiber was subjected to repeated heat treatments. The fiber heat treated at 85% of power (approximately 1780 °C) for 10 heating cycles is displayed in the SEM micrograph of Fig. 9. As shown in SEM micrographs, the heat treated fiber had facetted flat surfaces with surface steps. The diameter of the heat treated fiber was 97 μm, whereas the diameter of the green fiber was 150 μm. Thus the diameter shrank by about 65%. The EDS analysis showed that the composition of the heat treated mullite was $3Al_2O_3{:}2SiO_2$ with no trace of Ti. In mullite crystallization, when the mullite phase was formed from the melt, it has the $2Al_2O_3{\cdot}SiO_2$ composition, whereas when it was crystallized at a lower temperature, it has the 3:2 composition.[38] It is believed that the amount of Ti in the whiskers was less than the range detectable by TEM/EDS.

The heat treated fiber was examined by optical microscopy. Fig. 10 is a reflected light image of the heat treated fiber. The micrograph shows flat facets with steps as seen in the SEM micrograph (Fig. 9(b)). There was no total extinction direction when seen in crossed polarized lights. It is believed that the different crystallographic orientations of the flat surfaces and steps may prevent total extinction.

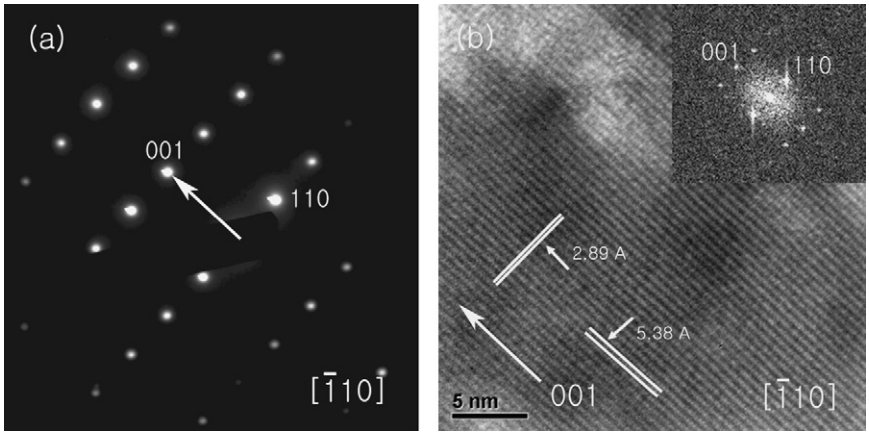

Fig. 12. TEM images of whisker-templated, mullite fiber heat-treated 10 times at 85% of power (approximately 1780 °C), at a transverse rate of 1 μm/s, (a) TEM diffraction pattern, and (b) high resolution of TEM image with projection zone was [$\bar{1}$ 1 0].

The facets on the heat treated fiber were ion milled for TEM specimen preparation. Fig. 11(a) shows the transmitted light image of an ion-milled fiber. In this bamboo-like section of the fiber, the sample was in total extinction in transmitted polarized light when the fiber was rotated parallel to the cross hairs, as seen in Fig. 11(b). The same segment of fiber was examined by TEM. Fig. 12 shows the TEM/SAD diffraction pattern of the heat-treated fiber. The projection zone was [−1 1 0] and diffraction patterns contained {0 0 1} and {1 1 0} reflections. The high resolution TEM image showed that the growth direction along the fiber length was along the [0 0 1] direction of orthorhombic mullite in that section of the fiber. The lattice parameters measured from the high resolution TEM micrograph corresponded to those reported for {0 0 1} and {1 1 0} planes of 3:2 mullite.

4. Conclusion

The feasibility of growing textured mullite fibers by heat treatment of polycrystalline fibers was demonstrated using the quadrupole lamp furnace. Mullite whiskers were prepared as templates for templated grain growth. The crystallite size growth rate and shape were examined by micrographic analysis and *in situ* synchrotron X-ray diffraction analysis. With the analysis by the Williamson–Hall method, the crystallites showed anisotropy. The growth rate along the *c*-axis was higher than in the [1 1 0] direction. Three weight percent of titania dopant was added to enhance elongated mullite grain growth. Repeated heat treatments of templated fibers resulted in mullite fiber with a bamboo-like microstructure consisting of large grains. The microstructure of one heat treated mullite fiber was examined by transmission electron microscopy. It was confirmed that the grown direction along the fiber length was the [0 0 1] direction of orthorhombic mullite. With an optical microscope in transmitted polarized light analysis, those bamboo-like grains showed total extinction along the fiber length direction.

Acknowledgements

This work was supported by the AFOSR under grant F49620-03-1-0082. Use of the facilities in the Center for Microanalysis of Materials, University of Illinois, which is partially supported by the US Department of Energy under grant DEFG02-91-ER45439 and the APS, Argonne National Laboratory is supported by the US DOE, BES-Materials Sciences, under Contract No: W-31-109-ENG-38 are gratefully acknowledged.

References

1. Bunsell, A. R. and Berger, M. H., Fine diameter ceramic fibres. *J. Eur. Ceram. Soc.*, 2000, **20**(13), 2249–2260.
2. Schneider, H., Thermal expansion of mullite. *J. Am. Ceram. Soc.*, 1990, **73**(7), 2073–2076.
3. Schneider, H., Pask, J. A. and Okada, K., *Mullite and mullite ceramics*. John Wiley, Chichester, NY, 1994.
4. Sundaresan, S. and Aksay, I. A., Mullitization of diphasic aluminosilicate gels. *J. Am. Ceram. Soc.*, 1991, **74**(10), 2388–2392.
5. Mroz, T. J. and Laughner, J. W., Microstructures of mullite sintered from seeded sol gels. *J. Am. Ceram. Soc.*, 1989, **72**(3), 508–509.
6. Petry, M. D. and Tai-Il, M., Effect of thermal exposures on the strengths of Nextel 550 and 720 filaments. *J. Am. Ceram. Soc.*, 1999, **82**(10), 2801–2807.
7. Mileiko, S. T., Kiiko, V. M., Starostin, M. Y., Kolchin, A. A. and Kozhevnikov, L. S., Fabrication and some properties of single crystalline mullite fibers. *Scrip. Mater.*, 2001, **44**(2), 249–255.
8. Johnson, B. R., Kriven, W. M. and Schneider, J., Crystal structure development during devitrification of quenched mullite. *J. Eur. Ceram. Soc.*, 2001, **21**(14), 2541–2562.
9. Xiao, Z. and Brian, S. M., The production of mullite fibers *via* inviscid melt-spinning (IMS). *Mater. Lett.*, 1998, **37**, 359–365.
10. Sayir, A. and Farmer, S. C., Directionally solidified mullite fibers. *MRS Symp. Proc.*, 1995, **365**, 11–20.
11. Ghate, B. B., Hasselmann, D. P. H. and Spriggs, R. M., Kinetics of pressure sintering and grain growth of ultra-fine mullite powder. *Ceram. Int.*, 1975, **1**, 105–110.
12. Huang, T. H., Rahaman, M. N., Mah, T. I. and Parthasarathay, T. A., Anisotropic grain growth and microstructural evolution of dense mullite above 1550 °C. *J. Am. Ceram. Soc.*, 2000, **83**(1), 204–210.
13. Michel, D., Mazerolles, L. and Portier, R., Directional solidification in the alumina-silica system microstructures and interfaces. In *Mullite and mullite matrix composites*, ed. S. Somiya, R. F. Davis and J. A. Pask, 1990, pp. 435–447.
14. Okada, K. and Otuska, N., Synthesis of mullite whiskers and their application in composites. *J. Am. Ceram. Soc.*, 1991, **74**(10), 2414–2418.
15. Hong, S. H. and Messing, G. L., Anisotropic grain growth in diphasic-gel-derived titania-doped mullite. *J. Am. Ceram. Soc.*, 1998, **81**(5), 1269–1277.
16. Klug, H. P. and Alexander, L. E., *X-ray diffraction procedures for polycrystalline and amorphous materials*. Wiley, New York, 1974.
17. Knapp, M., Joco, V., Baehtz, C., Brecht, H. H., Berghaeuser, A., Ehrenberg, H. *et al.*, Position-sensitive detector system OBI for high resolution X-ray powder diffraction using on-site readable image plates. *Nucl. Instrum. Meth. Phys. Res. Sect. A-Accel. Spectrom. Dect. Assoc. Equip.*, 2004, **521**(2/3), 565–570.
18. Sarin, P., Haggerty, R. P., Yoon, W., Knapp, M., Berghauser, A., Zschack, P., et al., A curved image plate detector system for high resolution synchrotron X-ray diffraction. J. Synch. Rad., in preparation.
19. Sarin, P., Haggerty, R. P., Yoon, W., Zschack, P., Knapp, M. and Kriven, W. M., Rapid in-situ ultra-high temperature investigations of ceramics using synchrotron X-ray diffraction. *Ceram. Eng. Sci. Proc.*, 2006, **27**(2), 313–324.
20. Sarin, P., Yoon, W., Jurkschat, K., Zschack, P., Kriven, W. M., Quadrupole lamp furnace for high temperature (up to 2050 K) synchrotron powder X-ray diffraction studies in air in reflection geometry. Rev. Sci. Instrum., 77(9), in press.
21. Siah, L. F., Kriven, W. M. and Schneider, J., *In situ*, high-temperature, synchrotron, powder diffraction studies of oxide systems in air, using a thermal-image furnace. *Mea. Sci. Technol.*, 2005, **16**, 1–8.
22. Siah, L. F., Schneider, J. and Kriven, W. M., *In situ*, in air, high temperature studies of oxide systems using the thermal-imaging technique. *Adv. X-ray Anal.*, 2003, **46**, 264–269.
23. Hong, S. H. and Messing, G. L., Development of textured mullite by templated grain growth. *J. Am. Ceram. Soc.*, 1999, **82**(4), 867–872.
24. Toby, B.H., CMPR—a multipurpose freeware program to display diffraction data, manual & auto indexing, peak fitting and other useful stuff; 2005.
25. Young, R. A., Mackie, P. E. and Dreele, R. B., Application of the pattern-fitting structure-refinement method to X-ray powder diffractometer patterns. *J. Appl. Crystallogr.*, 1977, **10**, 262–269.
26. Seabaugh, M. M., Kerscht, I. H. and Messing, G. L., Texture development by templated grain growth in liquid-phase-sintered alpha-alumina. *J. Am. Ceram. Soc.*, 1997, **80**(5), 1181–1188.
27. Okada, K., Yasohama, S., Hayashi, S. and Yasumori, A., Mullite long fibres prepared by sol–gel method using water solvent systems. *Key Eng. Mater.*, 1997, **132–136**(Pt), 1946–1949.
28. Schneider, H., Transition metal distribution in mullite. In *Mullite and mullite matrix composites*, ed. S. SOMIYA, R. F. Davis and J. A. Pask, 1990, pp. 135–158.
29. Song, K. C., Preparation of mullite fibers by the sol–gel method. *J. Sol–Gel Sci. Technol.*, 1998, **13**(1–3), 1017–1021.

30. Hwang, C. M., Tien, T. Y. and Chen, I. W., Anisotropic grain growth during final stage sintering of silicon nitride ceramics. In *Sintering '87*, ed. S. Somiya, M. Shimada and R. Watanabe, 1988, pp. 1034–1039.
31. Lai, K. R. and Tien, T. Y., Kinetics of beta-Si_3N_4 grain-growth in Si_3N_4 ceramics sintered under high-nitrogen pressure. *J. Am. Ceram. Soc.*, 1993, **76**(1), 91–96.
32. Seabaugh, M. M., Horn, D., Kerscht, I., Hong, S. H. and Messing, G. L., Anisotropic grain growth in alumina ceramics. In *Sintering technology*, ed. R. M. German, G. L. Messing and R. G. Cornwall, 1996, pp. 341–348.
33. Amigo, J. M., Serrano, F. J., Kojdecki, M. A., Bastida, J., Esteve, V. and Reventos, M. M., X-ray diffraction microstructure analysis of mullite, quartz and corundum in porcelain insulators. *J. Eur. Ceram. Soc.*, 2005, **25**(9), 1479–1486.
34. Williamson, G. K. and Hall, W. H., X-ray line broadening from filed aluminum and wolfram. *Acta Metallurg.*, 1953, **1**, 22–31.
35. Seabaugh, M. M., Suvaci, E., Brahmaroutu, B. and Messing, G. L., Modeling anisotropic single crystal growth kinetics in liquid phase sintered alpha-Al_2O_3. *Interface Sci.*, 2000, **8**(2–3), 257–267.
36. Suvaci, E., Simkovich, G. and Messing, G. L., The reaction-bonded aluminum oxide (RBAO) process: II, the solid-state oxidation of RBAO compacts. *J. Am. Ceram. Soc.*, 2000, **83**(8), 1845–1852.
37. Raj, R. and Ashby, M. F., On grain boundary sliding and diffusional creep. *Metall. Trans.*, 1971, **2**(4), 1113–1127.
38. Aksay, I. A., Dabbs, D. M. and Sarikaya, M., Mullite for structural, electronic, and optical applications. *J. Am. Ceram. Soc.*, 1991, **74**(10), 2343–2358.